Received: 7 October 2022 | Accepted: 24 November 2022

DOI: 10.1002/pamm.202200145

Linear and nonlinear thermoviscoelastic behavior of polyamide 6

Johannes Keursten[1,*], **Loredana Kehrer**[1], and **Thomas Böhlke**[1]

[1] Institute of Engineering Mechanics, Chair for Continuum Mechanics, Karlsruhe Institute of Technology (KIT), Karlsruhe, Germany

Thermoplastic polyamides are used in many industrial areas due to their potential in lightweight applications. Polyamides serve as matrix material in fiber reinforced thermoplastics, for instance. The mechanical behavior of polyamides is characterized by pronounced viscoelastic effects that are strongly affected by environmental conditions like temperature or humidity. In this work, linear thermoviscoelastic behavior of polyamide 6 is considered. Viscoelastic behavior is modeled by the generalized Maxwell model while extended time-temperature superposition is used to model temperature dependency. A temperature-frequency sweep conducted by dynamic mechanical analysis serves as input for the model. By horizontal and vertical shifting, master curves of the loss factor, storage modulus, and loss modulus are obtained. Based on this, limitations of time-temperature superposition and linear thermoviscoelastic modeling are discussed. Furthermore, it is shown that the horizontal shifts can be well approximated by the Williams-Landel-Ferry equation for temperatures above and below the glass transition temperature.

1 Introduction

Polymer-based materials are used in a broad range of industrial applications as they enable for cost-efficient production. As matrix material in fiber reinforced composites, polymers can be applied in high load-bearing components. In particular, thermoplastic polyamides are suited as matrix material in lightweight components due to high specific strengths and stiffnesses [1]. From mechanical perspective, polyamides exhibit pronounced viscoelastic behavior [2]. This behavior is strongly influenced by environmental conditions like temperature or humidity [3]. To describe linear viscoelastic behavior, rheological models are often used. In a strain-driven setup, for instance, the generalized Maxwell model (GMM) is commonly used [4, 5]. The GMM combines linear spring and dashpot elements that represent the stiffness and viscosity properties of the material. The resulting linear viscoelastic properties like relaxation modulus or storage and loss modulus depend on these stiffnesses and viscosities. A common approach to model temperature dependency of linear viscoelastic properties is based on thermorheological simplicity [4, 6]. In terms of a GMM, the viscosities are temperature-dependent properties while the stiffnesses are temperature-independent. The temperature dependency of all viscosities is given by a common shift function $a(\theta)$. On a logarithmic scale, this leads to a shift of the viscoelastic properties in the frequency or time domain (horizontal shift). This principle is called time-temperature superposition (TTS). TTS allows to combine experimental measurements at various temperature levels to master curves with larger frequency or time ranges. In literature, the shift function $a(\theta)$ is often described by the Williams-Landel-Ferry (WLF) equation or an Arrhenius equation [7, 8]. The WLF equation is mainly applicable for temperatures above the glass transition temperature θ_g. In contrast, the Arrhenius equation is used for temperatures lower than θ_g. In terms of temperature-dependent stiffnesses, horizontal shifting is not sufficient to obtain smooth master curves [9]. Then, TTS can be extended by introducing a vertical shift function $b(\theta)$ for the stiffnesses [10, 11]. On a logarithmic scale, this leads to an additional vertical shift. The neglection of vertical shifts can cause large errors in the master curves [4].
In this work, the thermoviscoelastic behavior of polyamide 6 (PA 6) is considered. The main objective is to identify limitations of linear thermoviscoelastic modeling of PA 6. Precisely, the focus is on modeling temperature dependency by extended TTS. An experimental temperature-frequency sweep conducted by dynamic mechanical analysis serves as input. The procedure of constructing master curves by horizontal and vertical shifting of frequency-dependent properties is described. The limitations of the temperature and frequency ranges for the TTS application are addressed. Additionally, a parameter identification for the WLF equation and the GMM is conducted. The work is seen as prework for a nonlinear thermoviscoelastic model.

2 Methods and Fundamentals

Linear viscoelasticity. In this work, a one-dimensional formulation of the GMM is considered as the experimental characterization is performed by uniaxial testing. The GMM is a parallel connection of an elastic spring element and an arbitrary number N of Maxwell elements. Each Maxwell element consists of a spring element and a dashpot element in series. Spring elements are given by stiffnesses $E_i,\ i = 0, \dots, N$, and dashpot elements are given by viscosities $\eta_i,\ i = 1, \dots, N$. Relaxation times of the Maxwell elements are defined by $\tau_i := \eta_i / E_i,\ i = 1, \dots, N$. The general stress response of a GMM to a strain load is

* Corresponding author: johannes.keursten@kit.edu

given by the Boltzmann superposition integral [4], reading

$$\sigma(t) = E_0\varepsilon(t) + \int_0^t \sum_{i=1}^{N} E_i \exp\left(-\frac{t-s}{\tau_i}\right) \dot{\varepsilon}(s)\mathrm{d}s. \tag{1}$$

In dynamic tests, samples are loaded by a cyclic strain with oscillation frequency ω, mean strain ε_0, and amplitude $\Delta\varepsilon$

$$\varepsilon(t) = \varepsilon_0 + \Delta\varepsilon \sin(\omega t), \quad \dot{\varepsilon}(t) = \Delta\varepsilon\, \omega \cos(\omega t). \tag{2}$$

The linear viscoelastic stress response is given by

$$\sigma(t) = \sigma_0 + \Delta\varepsilon \left(E' \sin(\omega t) + E'' \cos(\omega t)\right) = \sigma_0 + \Delta\varepsilon |E^*| \sin(\omega t + \delta). \tag{3}$$

Storage modulus E' and loss modulus E'' describe the elastic and the viscous part of the dynamic response, respectively. The absolute value of the dynamic modulus $|E^*|$ and the loss factor $\tan\delta$ are given by

$$|E^*| = \sqrt{E'^2 + E''^2}, \quad \tan\delta = \frac{E''}{E'}. \tag{4}$$

Inserting Eq. (2) into Eq. (1), solving the integral by partial integration, and comparing the coefficients yields

$$E'(\omega) = E_0 + \sum_{i=1}^{N} E_i \frac{(\omega\tau_i)^2}{1+(\omega\tau_i)^2}, \quad E''(\omega) = \sum_{i=1}^{N} E_i \frac{\omega\tau_i}{1+(\omega\tau_i)^2}. \tag{5}$$

Temperature dependency. The temperature dependency of linear viscoelastic properties is often modeled by assuming thermorheological simplicity [4]. This implicates that the stiffnesses do not depend on temperature, whereas the viscosities and relaxation times depend on temperature by the shift function $a(\theta)$ with prescribed reference temperature θ_{ref}

$$\tau_i(\theta) = a(\theta)\tau_i^{\mathrm{ref}}, \quad \tau_i(\theta_{\mathrm{ref}}) = \tau_i^{\mathrm{ref}}, \quad i = 1, \ldots, N. \tag{6}$$

On a logarithmic frequency scale, a temperature change leads to a horizontal shift of viscoelastic properties. This principle is called TTS. The reference temperature can be arbitrarely chosen. By TTS, experimental measurements of viscoelastic properties at a limited frequency range but various temperatures can be combined to master curves. This master curves describe the material's behavior for a broader frequency range. The WLF equation [12] is often used to describe the shift function

$$\log a(\theta) = -c_1 \frac{\theta - \theta_{\mathrm{ref}}}{c_2 + \theta - \theta_{\mathrm{ref}}}, \tag{7}$$

with the parameters $\{c_1, c_2\}$ that need to be fitted to experimental data. By adding a vertical shift, thermorheological simplicity can be extended. In this case, the stiffnesses depend on temperature by an additional shift function $b(\theta)$

$$E_i(\theta) = b(\theta)E_i^{\mathrm{ref}}, \quad E_i(\theta_{\mathrm{ref}}) = E_i^{\mathrm{ref}}, \quad i = 0, \ldots, N. \tag{8}$$

All in all, the temperature-dependent storage and loss modulus are then given by

$$E'(\omega,\theta) = b(\theta)\left(E_0 + \sum_{i=1}^{N} E_i \frac{(a(\theta)\omega\tau_i)^2}{1+(a(\theta)\omega\tau_i)^2}\right), \quad E''(\omega,\theta) = b(\theta)\sum_{i=1}^{N} E_i \frac{a(\theta)\omega\tau_i}{1+(a(\theta)\omega\tau_i)^2}. \tag{9}$$

Experimental testing. A temperature-frequency sweep is performed by dynamic mechanical analysis (DMA) to obtain frequency- and temperature-dependent viscoelastic properties of PA 6. The testing device GABO Eplexor®500N is used. A dry-as-molded (DAM) sample is tested under varying frequency and temperature load ($0.5\,\mathrm{Hz} - 50\,\mathrm{Hz}$, $0°\mathrm{C} - 200°\mathrm{C}$). Mean strain and strain amplitude are set to $\varepsilon_0 = 0.1\%$ and $\Delta\varepsilon = 0.05\%$, respectively. Amplitude and phase shift δ of the stress response are measured. Then, storage modulus, loss modulus, and loss factor can be determined by Eq. (3) and Eq. (4).

Determination of shift factors. The DMA measurements of the viscoelastic properties are used as input for the construction of master curves. Horizontal and vertical shifts are determined by a sequential method based on the work of [13]. Relative shifts between curves of neighbouring temperature levels are calculated by an arc length minimization. First, the horizontal shift is determined based on the loss factor. Then, vertical shifts are calculated based on the storage modulus if needed.

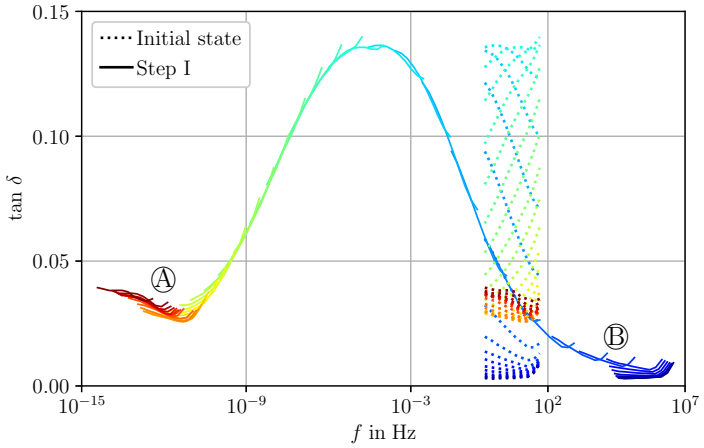

Fig. 1: Horizontal shifting is applied to the loss factor data. The unshifted data is depicted by the dotted curves (initial state). These curves are horizontally shifted to the solid lines (step I). From the blue to the red lines, temperature is increasing from $0^\circ\mathrm{C}$ to $200^\circ\mathrm{C}$. The reference temperature is set to $\theta_{\mathrm{ref}} = 50^\circ\mathrm{C}$.

Parameter identification. Based on the resulting master curves of storage and loss modulus, parameters of a GMM can be identified. To avoid an ill-posed problem, the relaxation times are prescribed logarithmically distributed [14]. Then, $N+1$ stiffnesses are identified by minimizing the least squares residual

$$r^2(\mathcal{P}_N) = \sum_{i=1}^{n_\omega} \left(\frac{E_i' - E'(\omega_i, \mathcal{P}_N)}{E_i'} \right)^2 + \sum_{i=1}^{n_\omega} \left(\frac{E_i'' - E''(\omega_i, \mathcal{P}_N)}{E_i''} \right)^2, \quad \mathcal{P}_n = \{E_0, E_1, \ldots, E_N\} \tag{10}$$

The number of data points of each master curve is denoted by n_ω. Storage modulus $E'(\omega_i, \mathcal{P}_N)$ and loss modulus $E''(\omega_i, \mathcal{P}_N)$ are given by Eq. (5). A gradient-based optimization method is used to solve the problem.

3 Results

Horizontal shifting. In this section, the construction of the master curves is discussed. In the first iteration, horizontal shifts are determined for the whole set of experimental data for the loss factor to identify limitations of TTS. The reference temperature θ_{ref} is set to $50^\circ\mathrm{C}$. In Fig. 1, the dotted lines represent the measured $\tan\delta(\omega)$ curves at various temperature levels (initial state). The solid lines depict the horizontally shifted curves (step I) where the temperature is increasing from right to left. A smooth master curve should be obtained in domains where TTS is applicable. In general, all partial curves deviate from the master curve at higher physical frequencies (at the right) due to an increase of the loss factor. Thus, the measurements for $f > 20$ Hz are not considered in the second iteration. Furthermore, for the highest and lowest temperatures, TTS is also not applicable, see Fig. 2. The domains of the highest and lowest temperatures are magnified on the left and on the right, respectively. For the highest temperatures, no smooth master curve can be obtained by the shift method. By neglecting the highest frequencies of the partial curves for $\theta \leq 130^\circ\mathrm{C}$, a smooth curve is expected in the second iteration. The curves at $\theta > 130^\circ\mathrm{C}$ will not be considered in the second iteration. For the four lowest temperatures, the partial curves are nearly constant if the highest frequencies are neglected. Thus, horizontal shifting does not result in a smooth master curve. The measurements for $\theta < 20^\circ\mathrm{C}$ will not be considered in the second iteration. In Fig. 3, the result of the second iteration is depicted. A smooth master curve is obtained for the loss factor.

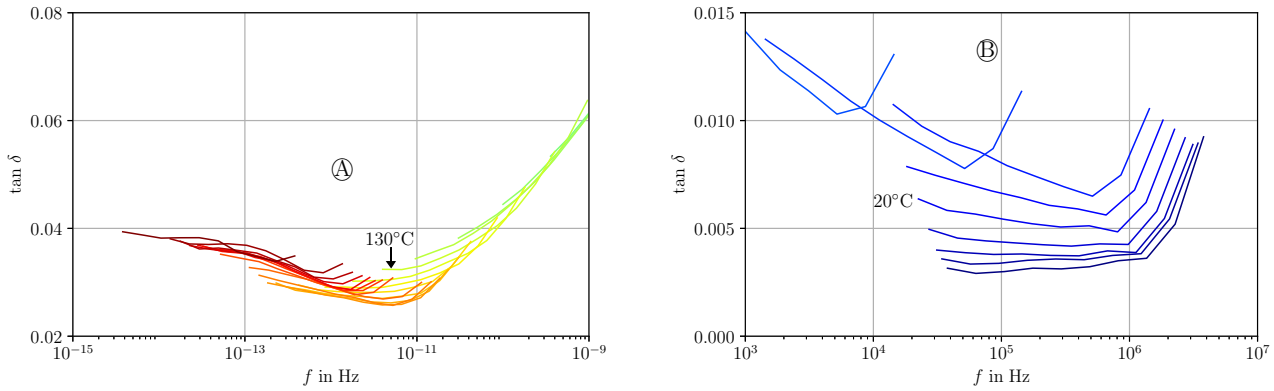

Fig. 2: Magnification of the domains from Fig. 1, where TTS is not applicable. For the highest temperatures on the left plot and the lowest temperatures on the right plot, no smooth master curve of the loss factor is obtained.

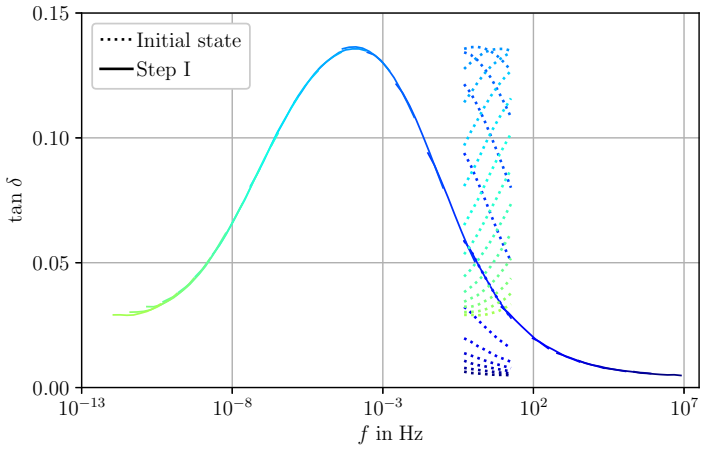

Fig. 3: Master curve of the loss factor obtained by horizontal shifting after restricting to $f < 20$ Hz and $20°\mathrm{C} \leq \theta \leq 130°\mathrm{C}$. The reference temperature is set to $\theta_{\mathrm{ref}} = 50°\mathrm{C}$. The color scheme used here coincides with the scheme used in Fig. 1

.

WLF equation. In Fig. 4, the horizontal shifts from Fig. 3 are depicted in black. These data points are considered for a fit of the WLF equation with the parameters $\{c_1, c_2\}$. The parameter identification is conducted by least squares optimization. For the considered temperature range, the resulting curve is shown in red. The behavior of the horizontal shifts is captured well by the parameter fit. This includes temperatures above and below the glass transition temperature of $75°\mathrm{C}$. Thus, a piecewise distinction between a WLF equation and an Arrhenius equation is not necessary here.

Vertical shfiting. Next, the horizontal shift is applied to storage modulus and loss modulus. The result is depicted by the dashed lines in Fig. 5 and Fig. 6. Especially for lower temperatures, the partial curves do not form a smooth master curve. Therefore, vertical shifts are necessary. The vertical shifts are determined based on the storage modulus resulting to the solid lines. In Fig. 6, the calculated shifts are applied to the loss modulus. Both storage and loss modulus show smooth master curves after horizontal and vertical shifting. The loss factor is not affected by a vertical shift, as it is defined as ratio of loss modulus to storage modulus, see Eq. (4) and Eq. (9).

Parameter identification. The master curves from Fig. 5 and Fig. 6 are used as input for a parameter identification of the GMM, see Eq. (10). A number of 40 Maxwell elements is used which are two elements per frequency decade. In Fig. 7, the predicted behavior based on the parameter identification is shown by the blue and the red curve for E' and E'', respectively. Both master curves are well approximated.

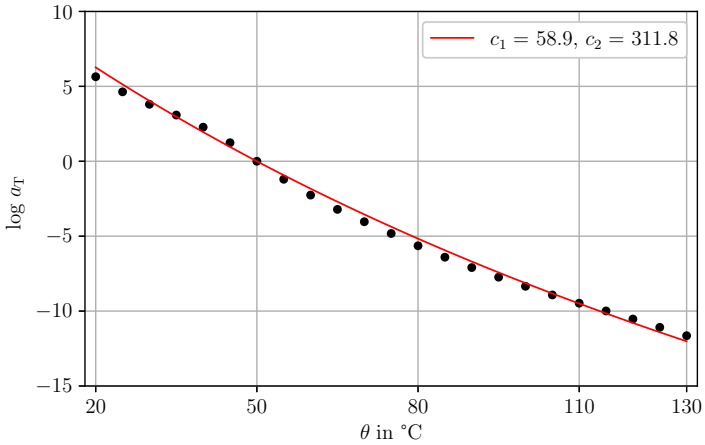

Fig. 4: The horizontal shift factors depicted by black points are fitted to the WLF equation (7). The fit is accurate within the considered temperature range.

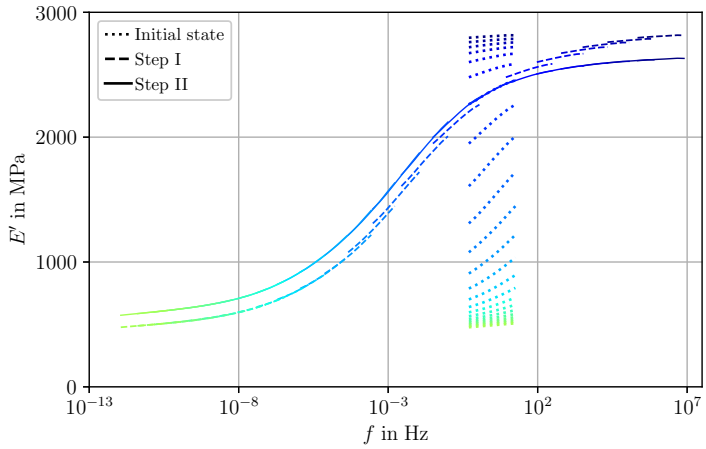

Fig. 5: Horizontal and vertical shifting is applied to the storage modulus data. Unshifted data is depicted by the dotted curves. The dashed curves result after horizontal shifting (step I). The solid lines show the final state after adding vertical shifts (step II).

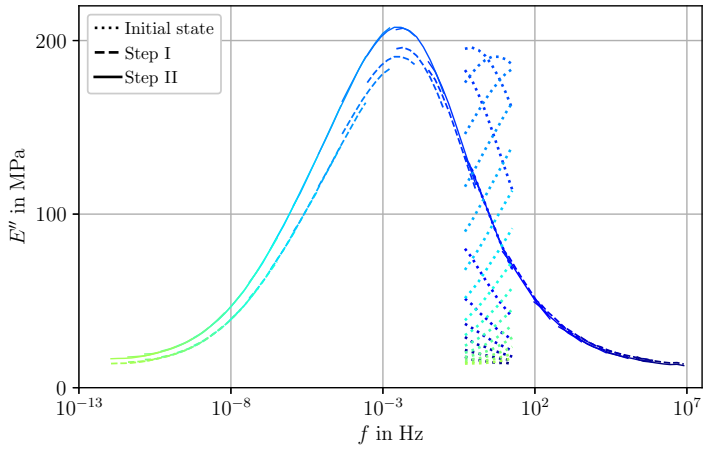

Fig. 6: Horizontal and vertical shifts determined by loss factor and storage modulus data, respectively, is applied to the loss modulus data. Unshifted data is depicted by the dotted curves. The dashed curves result after horizontal shifting (step I). The solid lines show the final state after adding vertical shifts (step II).

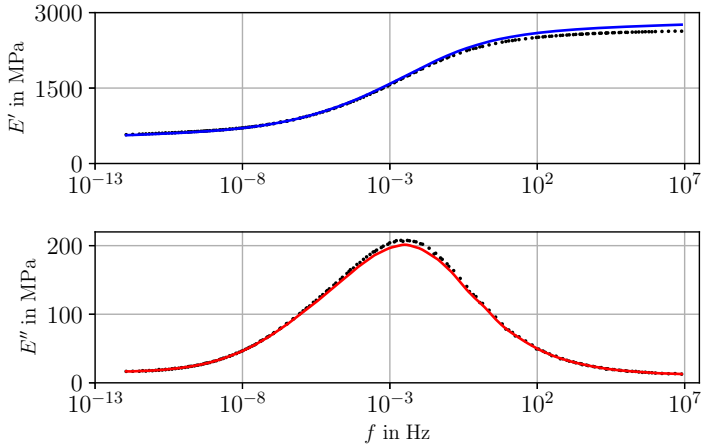

Fig. 7: The black points depict the experimentally determined master curves of storage and loss modulus. By least squares optimization, parameters are identified for a GMM with 40 Maxwell elements. The result is depicted by the blue and the red curve, respectively, showing good agreement between simulation results and experimental data.

4 Summary and conclusion

In this work, temperature dependency in the linear viscoelastic regime was modeled by extended TTS. In this context, frequency sweeps conducted at various temperatures by dynamic mechanical analysis were combined to master curves by horizontal and vertical shifting. First, horizontal shifts were determined based on the loss factor. In the first iteration, limitations of TTS were identified: $f < 20$ Hz, $20°\mathrm{C} \leq \theta \leq 130°\mathrm{C}$. In a second iteration, the master curve for the reduced set of data was constructed. The corresponding horizontal shifts can be described by the WLF equation for temperatures above and below the glass transition temperature. Second, smooth master curves were obtained for the storage modulus and the loss modulus by adding vertical shifts. The resulting master curves of the storage modulus and the loss modulus were used as input for a parameter identification. A linear GMM with two Maxwell element per frequency decade approximates the master curves of both storage and loss modulus well. Outside the range where TTS is applicable, nonlinear thermoviscoelastic models are needed. This is part of future scope of research.

Acknowledgements The research documented in this manuscript has been funded by the Deutsche Forschungsgemeinschaft (DFG, German Research Foundation), project number 255730231, within the International Research Training Group "Integrated engineering of continuous-discontinuous long fiber reinforced polymer structures" (GRK 2078/2). The support by the German Research Foundation (DFG) is gratefully acknowledged. Open access funding enabled and organized by Projekt DEAL.

Author contributions

Johannes Keursten: Conceptualization; methodology; simulation; writing - original draft
Loredana Kehrer: Experiments; writing - editing and review
Thomas Böhlke: Supervision; funding acquisition; writing - editing and review

References

[1] H. Domininghaus, Kunststoffe: Eigenschaften und Anwendungen (Springer, Berlin, 2012).
[2] G. Ehrenstein, Polymer-Werkstoffe (Hanser-Verlag, München, 2011).
[3] M. Stommel, M. Stojek, and W. Korte, FEM zur Berechnung von Kunststoff- und Elastomerbauteilen (Hanser, München, 2018).
[4] H. Brinson and L. Brinson, Polymer Engineering Science and Viscoelasticity: An Introduction (Springer, New York, 2015).
[5] A. Serra-Aguila, J. Puigoriol-Forcada, G. Reyes, and J. Menacho, Acta Mechanica Sinica **35**(6), 1191–1209 (2019).
[6] J. Ferry, Viscoelastic Properties of Polymers (John Wiley & Sons, New York, 1980).
[7] K. G. N. C. Alwis and C. J. Burgoyne, Applied Composite Materials **13**(4), 249–264 (2006).
[8] A. Serra-Aguila, J. Puigoriol-Forcada, G. Reyes, and J. Menacho, Polymers **14**(6), 1–18 (2022).
[9] J. Capodagli and R. Lakes, Rheologica Acta **47**(7), 777–786 (2008).
[10] J. Dealy and D. Plazek, Rheology Bulletin **78**(2), 16–31 (2009).
[11] L. Rouleau, J. F. Deü, A. Legay, and F. Le Lay, Mechanics of Materials **65**, 66–75 (2013).
[12] M. Williams, R. Landel, and J. Ferry, Journal of the American Chemical Society **77**(14), 3701–3707 (1955).
[13] J. E. Bae, K. S. Cho, K. H. Seo, and D. G. Kang, Korea-Australia Rheology Journal **23**(2), 81–87 (2011).
[14] R. Bradshaw and L. Brinson, Mechanics of Time-Dependent Materials **1**(1), 85–108 (1997).

